ISSN 0208-7774 TRIBOLOGIA 3/2019 p. 19–29
DOI: 10.5604/01.3001.0013.5430

Sławomir BEDNARCZYK[*], Ludomir JANKOWSKI[**], Justyna KRAWCZYK[***]

THE INFLUENCE OF ECCENTRICITY CHANGES ON POWER LOSSES IN CYCLOIDAL GEARING

WPŁYW ZMIAN MIMOŚRODOWOŚCI NA STRATY MOCY W ZAZĘBIENIU CYKLOIDALNYM

Key words: cycloidal gearing, power losses, clearance.

Abstract Gearing is one of the most important rolling nodes in a cycloidal planetary transmission. It consists of gears whose outlines are created according to cycloidal curves and the rollers cooperating with them. The epicycloidal and hypocycloidal gearing can be distinguished. There are power losses during the transmission operation, due to the transmitted load and friction in the gearing. The paper presents an analytical method for determining losses in cycloidal gearing, taking into account the manufacturing deviations of the elements making this gearing. The analysis allowed determining the distribution of intertooth clearances and forces at the points of contact between the profiles and the rollers, and consequently the distribution of power losses in gearing. The distribution of intertooth forces was verified by elastooptic tests of the gears set with cycloidal gearing. The results of the calculations indicate that the influence of eccentricity changes on the distribution of intertooth forces is significant and also that the distribution of power losses in gearing is closely related to the distribution of intertooth forces and has a very similar character.

Słowa kluczowe: zazębienie cykloidalne, straty mocy, luz.

Streszczenie Zazębienie jest jednym z ważniejszych węzłów tocznych w obiegowej przekładni cykloidalnej. Składa się ono z kół, których zarysy utworzone są wg krzywych cykloidalnych, oraz ze współpracujących z nimi rolek. Rozróżnia się zazębienie epicykloidalne i hipocykloidalne. Podczas pracy przekładni na skutek przenoszonego obciążenia oraz tarcia w zazębieniu występują straty mocy. W pracy przedstawiono metodę analityczną wyznaczania strat w zazębieniu cykloidalnym z uwzględnieniem odchyłek wykonawczych elementów tworzących to zazębienie. Przeprowadzona analiza pozwoliła na wyznaczenie rozkładu luzów międzyzębnych oraz sił w miejscach styku zarysów z rolkami, a w konsekwencji rozkładu strat mocy w zazębieniu. Rozkład sił międzyzębnych zweryfikowano poprzez badania elastooptyczne zespołu kół z zazębieniem cykloidalnym. Wyniki przeprowadzonych obliczeń wskazują, że wpływ zmian mimośrodowości na rozkład sił międzyzębnych jest istotny. A także, że rozkład strat mocy w zazębieniu ma ścisły związek z rozkładem sił międzyzębnych i ma bardzo podobny charakter.

INTRODUCTION

Planetary transmissions with cycloidal gearing are commonly used as basic units in drive systems. They are characterized by a high ratio, high efficiency, and small overall dimensions. During the operation of the transmission, the gearing transmits torque which results in the generation of intertooth forces and rolling friction. Both forces and friction in the gearing are responsible for the power losses affecting the overall efficiency of the transmission. The intertooth forces in the clearance-free transmissions and for the nominal gearing are determined by analytical methods [**L. 1**]. In turn, numerical methods allow one to determine the forces

[*] ORCID: 0000-0002-7266-344X. Wrocław University of Science and Technology, Department of Fundamentals Machine Design and Tribology, I. Łukasiewicza 5 Street, 50-371 Wrocław, Poland.
[**] ORCID: 0000-0002-3216-6641. Wrocław University of Science and Technology, Department of Biomedical Engineering, Mechatronics and Theory of Mechanisms, I. Łukasiewicza 5 Street, 50-371 Wrocław, Poland.
[***] ORCID: 0000-0002-5901-9289. Wrocław University of Science and Technology, Department of Fundamentals Machine Design and Tribology, I. Łukasiewicza 5 Street, 50-371 Wrocław, Poland.

for the corrected gearing [**L. 2**]. Forces and stresses are also determined by numerical methods using the finite element method [**L. 3–4**]. Then it is possible to consider the deformability of all elements making the gearing, which is not possible in analytical methods. However, the gearing elements are made with a certain tolerance, which results in clearances. As a result of these clearances, the distribution of forces in the gearing changes, and thus the power losses are also changed. In [**L. 5–7**], the influence of manufacturing tolerances of the transmission's elements on the intertooth clearance was determined. Analytical methods also allow one to determine the intertooth forces, taking into account the clearances in gearing [**L. 8**]. While [**L. 9**] presents a generalized dynamic contact model of elements making the epicycloid gearing. The model includes the same intertooth clearance in all teeth pairs. The numerical simulation showed the influence of the geometry of the gearing and the clearance occurring in it on the distribution of intertooth forces.

As already mentioned, friction in the gearing affects the efficiency of the transmission [**L. 10**]. It can be determined in an analytical or experimental way. In [**L. 11**], two analytical methods for determining the efficiency of a cycloidal transmission were compared with each other. The authors of [**L. 12–13**] analysed the influence of geometrical and material parameters on power losses in the clearance-free transmissions.

In this work, the goal was to determine the power losses in the cycloidal gearing (epi- and hypo), taking into account the manufacturing deviations of its elements and analysis of the impact of eccentricity changes, e.g., (eccentricity manufacturing deviation of the active shaft) on these losses. Therefore, the distribution of the clearances and forces occurring in the gearing and finally the power losses in the individual teeth pairs were determined. The analysis was carried out for many cases, taking into account different gearing geometries (number of teeth of the planetary gear and roller diameters), load values, and manufacturing deviations, which allowed the presentation of general distributions of clearances, forces, and power losses.

INTERTOOTH CLEARANCES

Cycloidal curves are commonly used in planetary gear transmissions, usually operating as reducers. Teeth profiles formed according to these curves together with the rollers are used in making cycloidal gearing. Epicycloidal and hypocycloidal gearing can be distinguished [**L. 14**], which is shown in **Fig. 1**. The epicycloidal gearing consists of a planetary gear eccentrically mounted on the active shaft, with an epicycloidal tooth profile and rollers located in the body sockets. In turn, the hypocycloidal gearing is made of rollers located in the sockets of the planetary gear, cooperating with the hypocycloidal outline of central gear, acting as a body. Each roller with the outline of the gear creates a pair of teeth. These elements are made separately and with certain, assumed tolerance. Therefore, there may be an intertooth clearance Δ_i between them. **Fig. 1** also shows the tolerances for the individual elements that have an impact on the creation of the intertooth clearance Δ_i for both types of gearing.

Therefore, the following can be distinguished [**L. 8**]:

- The tolerance of the planetary gear outline – T_{ze} (**Fig. 1a**);
- The tolerance of the central gear outline – T_{zh} (**Fig. 1b**);
- The tolerance of the roller – T_r;
- The tolerance of the rollers arrangement radius in the body – T_{Rg};
- The tolerance of the angular arrangement of rollers in the body – $T_{\varphi R}$; and,
- The tolerance of the eccentricity – T_e.

a) b)

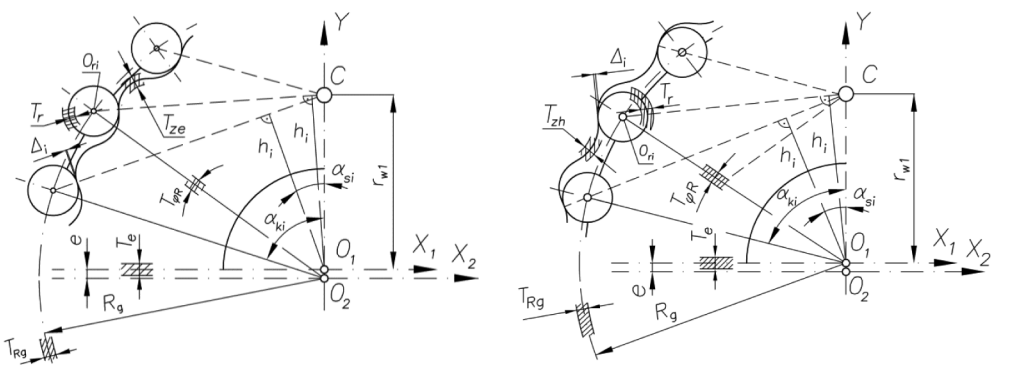

Fig. 1. Gearing tolerances: a) epicycloidal, b) hypocycloidal
Rys. 1. Tolerancje wykonania zazębienia: a) epicykloidalnego, b) hipocykloidalnego

Intertooth clearance Δ_i is determined along the direction of the intertooth forces F_i coming down in the pole of gearing C, as shown in **Fig. 2**. Thus, the force F_i lines are guided from the centre of the roller O_{ri} to the pole of gearing C.

On the basis of **Fig. 2a**, the intertooth clearance Δ_i for epicycloidal gearing can be specified as follows:

$$\Delta_i = \sqrt{\left(x_{ze} - x_{ozri}\right)^2 + \left(y_{ze} - y_{ozri}\right)^2} - \left(r_r + \delta_{rr}\right) \tag{1}$$

where

r_r – roller radius with manufacturing deviation δ_{rr}. This deviation is within tolerance T_r.

A fixed coordinate system $X_1 0_1 Y$ is associated with the planetary gear (**Fig. 2a**). The actual outline of the planetary gear, with a manufacturing deviation δ_{ze} from theoretical, can be described in the following way:

$$\begin{aligned} x_{ze} &= \rho \cdot (z+1) \cdot \cos\eta - \lambda \cdot \rho \cdot \cos\left((z+1)\right) \\ &\eta - (g - \delta_{ze}) \cdot \frac{\cos\eta - \lambda \cdot \cos\left((z+1)\eta\right)}{\sqrt{1 - 2 \cdot \lambda \cdot \cos z\eta + \lambda^2}} \\ y_{ze} &= \rho \cdot (z+1) \cdot \sin\eta - \lambda \cdot \rho \cdot \sin\left((z+1)\eta\right) \\ &- (g - \delta_{ze}) \cdot \frac{\sin\eta - \lambda \cdot \sin\left((z+1)\eta\right)}{\sqrt{1 - 2 \cdot \lambda \cdot \cos z\eta + \lambda^2}} \end{aligned} \tag{2}$$

a) b)

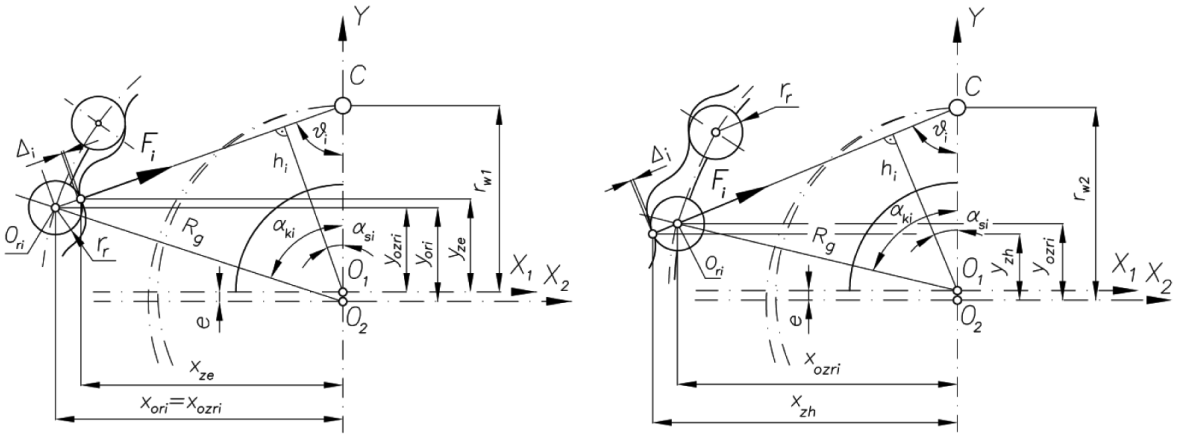

Fig. 2. Determination of intertooth clearances Δ_i: a) epicycloidal gearing, b) hypocycloidal gearing
Rys. 2. Wyznaczenie luzu międzyzębnego Δ_i: a) zazębienie epicykloidalne, b) zazębienie hipocykloidalne

The deviation δ_{ze} is within tolerance T_{ze}.

The movable coordinate system $X_2 0_2 Y$ is connected with the rollers **(Fig. 2a)**. In this system, coordinates x_{0ri}, y_{0ri} of the centre O_{ri} i-th roller can be described as follows:

$$\begin{aligned} x_{ori} &= \left(R_g + \delta_{Rg}\right) \cdot \sin\left(\varphi_{Ri} + \delta_{\varphi Ri}\right) \\ y_{ori} &= \left(R_g + \delta_{Rg}\right) \cdot \cos\left(\varphi_{Ri} + \delta_{\varphi Ri}\right) \end{aligned} \tag{3}$$

where

$$\varphi_{Ri} = \alpha_{ki} = \frac{2 \cdot \pi \cdot (i-1)}{z+1} \tag{4}$$

δ_{Rg} – manufacturing deviation of the rollers arrangement radius R_g;

$\delta_{\varphi Ri}$ – manufacturing deviation of the angular φ_{Ri} arrangement of the rollers.

These deviations are within tolerances T_{Rg} and $T_{\varphi R}$.

To determine the position of the centre of the roller O_{ri} in coordinate system $X_1 0_1 Y$, that is the coordinates of the planetary gear, transformational formulas should be used:

$$\begin{aligned} x_{ozri} &= x_{ori} \\ y_{ozri} &= y_{ori} - \left(e + \delta_e\right) \end{aligned} \tag{5}$$

where

δ_e – position error (eccentricity e) of the horizontal axis of the gear with cycloidal outline, relative to the axis of the cooperating gear.

This deviation is within tolerance T_e and is the result of manufacturing of eccentricity of active shaft, mounting on it planetary gear and placing it relative to the cooperating gear.

Using, in turn **Fig. 2b**, intertooth clearance Δ_i for hypocycloid gearing can be determined by the expression:

$$\Delta_i = \sqrt{\left(x_{zh} - x_{ozri}\right)^2 + \left(y_{zh} - y_{ozri}\right)^2} - \left(r_r + \delta_{rr}\right) \quad (6)$$

where

r_r – roller radius with manufacturing deviation δ_{rr}.

This deviation is within tolerance T_r.

A fixed coordinate system $X_2 0_2 Y$ is associated with the central gear (**Fig. 2b**). The actual outline of the central gear, with a manufacturing deviation δ_{zh} from theoretical, can be described in the following way:

$$\begin{aligned} x_{zh} &= \rho \cdot (z-1) \cdot \cos\eta + \lambda \cdot \rho \cdot \cos(z-1)\eta + \\ &+ (g + \delta_{zh}) \cdot \frac{\cos\eta - \lambda \cdot \cos(z-1)\eta}{\sqrt{1 - 2 \cdot \lambda \cdot \cos z\eta + \lambda^2}} \\ y_{zh} &= \rho \cdot (z-1) \cdot \sin\eta - \lambda \cdot \rho \cdot \sin(z-1)\eta + \\ &+ (g + \delta_{zh}) \cdot \frac{\sin\eta + \lambda \cdot \sin(z-1)\eta}{\sqrt{1 - 2 \cdot \lambda \cdot \cos z\eta + \lambda^2}} \end{aligned} \quad (7)$$

The deviation δ_{zh} is within tolerance T_{zh}.

The movable coordinate system $X_1 0_1 Y$ is connected with the rollers, placed in planetary gear (**Fig. 2b**). In this system, coordinates x_{ori}, y_{ori} of the centre O_{ri} i-th roller can be described as follows:

$$\begin{aligned} x_{ori} &= \left(R_g + \delta_{Rg}\right) \cdot \sin\left(\varphi_{Ri} + \delta_{\varphi Ri}\right) \\ y_{ori} &= \left(R_g + \delta_{Rg}\right) \cdot \cos\left(\varphi_{Ri} + \delta_{\varphi Ri}\right) \end{aligned} \quad (8)$$

To determine the position of the centre of the roller O_{ri} in coordinate system $X_2 0_2 Y$, that is the coordinates of the central gear, transformational formulas should be used:

$$\begin{aligned} x_{ozri} &= x_{ori} \\ y_{ozri} &= y_{ori} + \left(e + \delta_e\right) \end{aligned} \quad (9)$$

INTERTOOTH FORCES

During the operation of the reducer, torque M_K is created and it is affecting the planetary gear. This torque generates intertooth forces F_i occurring between the rollers and the outline of the gear in contact with them. The distribution of forces is shown in **Fig. 3**. In the clearance-free reducer, torque M_K is transmitted by half from all teeth pairs. In the case of transmissions with intertooth clearance Δ_i, the number of teeth pairs cooperating with each other varies depending on the size of this clearance.

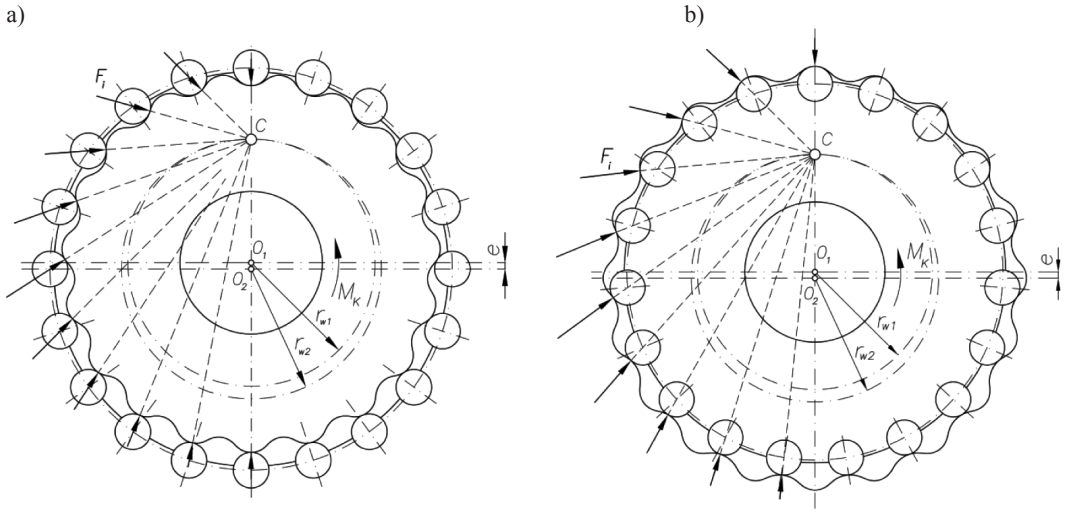

Fig. 3. Distribution of intertooth forces F_i: a) epicycloidal gearing, b) hypocycloidal gearing
Rys. 3. Rozkład sił międzyzębnych F_i: a) zazębienie epicykloidalne, b) zazębienie hipocykloidalne

In order to determine intertooth forces F_i the following assumptions were made:

- The gearing is nominal (uncorrected);
- The deformations of the planetary gear are not taken into account;
- Loads are evenly distributed on all planetary gears;
- Clearances Δ_i in the transmission occurs only between individual rollers and the cycloidal outline;
- The load is transferred only by one active side of the planetary gear, wherein the directions of forces acting on individual teeth form a set of straight lines intersecting at the point of contact C (the pole of gearing), as shown in **Fig. 3**;
- Displacement δ_i in the place of force F_i action, results from the small angular displacement of the planetary gear in a form of a rigid disc and are caused by the deflection of the rollers; and,
- Omitting the deformation of all elements of the cycloidal transmission (planetary gear, bearings, shaft, transmission body), it is assumed, that the intertooth force F_i is directly proportional (linearly dependent) to deformation (deflection) δ_i of the roller.

The torque M_K is balanced by coplanar intertooth force system F_i acting on arms h_i. Taking into account clearance Δ_i resulting from the tolerances of the individual elements of the transmission, it can be said that the intertooth force F_i acting in the teeth pairs is the following [**L. 8**]:

$$F_i = M_K \cdot \frac{(\delta_i - \Delta_i)}{\sum_{i=1}^{i=z_C} (\delta_i - \Delta_i) \cdot h_i} \quad (10)$$

,

where

δ_i – displacement of the centre of the roller O_{ri} due to its deflection [**L. 15–17**];

h_i – arm of force F_i [**L. 18–19**].

In the case when $\delta_i - \Delta_i < 0$, it is assumed that the roller is not in contact with the outline of the cooperating gear in a given teeth pair, i.e. F_i=0.

POWER LOSSES

Analysing the principle of the cycloidal transmission operation, it can be noticed that when the planetary gear rotates at an angular speed ω_k, while the roller rotating around its own axis at an angular speed ω_r simultaneously cooperates with the cycloidal outline and the socket in which it is located. Therefore, the power losses in a pair of gears with cycloidal outline and roller N_{Ck-r} is determined based on the following formula [**L. 13**]:

$$N_{Ck-r} = N_{Tk-r} + N_{Tr-o} \quad (11)$$

where

N_{Tk-r} – power losses between the cycloidal gear outline and the roller;

N_{Tr-o} – power loss between the roller and the socket.

The power of rolling friction losses occurring between the roller and the cycloidal outline can be determined as follows:

$$N_{Tk-r} = \sum_{i=1}^{i=z_C} F_i \cdot f_{k-r} \cdot (\omega_k + \omega_{ri}) \quad (12)$$

where

f_{k-r} – coefficient of rolling friction between the roller and the gear profile.

Assuming that the rolling point C is the instantaneous centre of the rotation of the planetary gear, and, assuming that there is no slip at the points of contact of the rollers with cycloid gearing (point A_i), the angular speed ω_{ri} of roller is as follows:

– For epicycloidal gearing:

$$\omega_{ri} = \omega_k \cdot \frac{\overline{CA_i}}{r_r + \delta_{rr}} \quad (13)$$

,

– For hypocycloidal gearing:

$$\omega_{ri} = \frac{(\overline{CA_i} - 2 \cdot r_r)}{2 \cdot r_r} \cdot \omega_k \quad (14)$$

where

$\overline{CA_i}$ – distance of the roller contact point A_i with the cycloidal outline from the rolling point C.

The relationship of the angular speed ω_0 of the input shaft to the angular speed ω_k of the planetary gear is as follows:

$$\omega_k = \omega_0 \cdot \frac{e}{r_{w1}} \quad (15)$$

where

r_{w1} – rolling radius of the planetary gear.

The power of rolling friction losses between the roller and the socket in the gear N_{Tr-o} is determined by the dependence:

$$N_{Tr-o} = \sum_{i=1}^{i=z_C} F_i \cdot f_{r-o} \cdot \omega_{ri} \quad (16)$$

where

f_{r-o} – coefficient of rolling friction between the roller and the socket in the planetary gear.

CALCULATION RESULTS

Using formulas (6), (10), (11), (12), and (16), it is possible to determine the influence of eccentricity deviation δ_e on the form of the intertooth clearance distribution Δ_i, the intertooth forces F_i dependent on it and finally the power losses N_{ck-r} in gearing. The analysis was carried out for many cases taking into account different gearing geometries (number of teeth in the planetary gear and roller diameters), load values, and manufacturing deviations. In all cases, the distribution of clearances Δ_i, forces F_i and power losses N_{ck-r} in gearing were very close to each other in qualitative terms. In each gearing, only eccentricity deviation δ_e was considered along with the manufacturing deviation of the cycloidal outline. It is necessary to take into account the outline deviation in order to obtain intertooth clearance $\Delta_i > 0$ in all teeth pairs and because it is the most technologically difficult element of gearing to be made. Thus, this is deviation δ_{ze} for the epicycloidal outline and deviation δ_{zh} for the hypocycloidal outline. Outline deviations with positive and negative values were considered. Fixed deviation values were assumed on the entire circuit of the gear profiles. As rollers in the shape of cylinders, being the second element of gearing, rolling elements of rolling bearings are commonly used. Usually they are made with smaller deviations, and they have a similar effect on the intertooth clearance Δ_i as the outline. **Fig. 4** shows the influence of eccentricity deviation δ_e and deviation of the outline δ_{ze} on the clearance distribution

a) b)

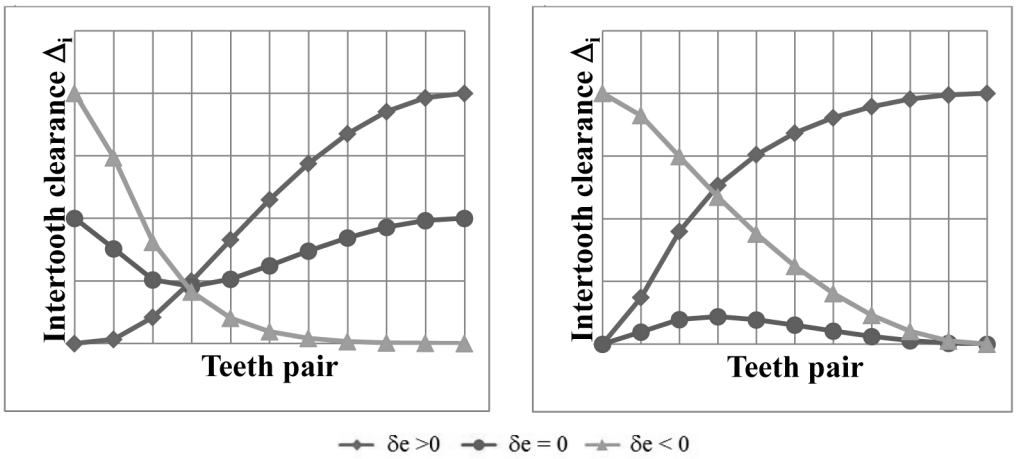

Fig. 4. The distribution of intertooth clearances Δ_i for epicycloidal gearing with: a) a positive deviation δ_{ze}, b) a negative deviation δ_{ze}

Rys. 4. Rozkład luzów międzyzębnych Δ_i dla epicykloidalnego zazębienia z: a) dodatnią jego odchyłką δ_{ze}, b) ujemną jego odchyłką δ_{ze}

Δ_i for epicycloidal gearing. **Fig. 5** shows the influence of eccentricity deviation δ_e and deviation of the outline δ_{zh} for hypocycloidal gearing. The distributions were constructed in such a way that, for each teeth pair, an intertooth clearance was determined Δ_i and plotted on the chart. The same was done with the distribution of intertooth forces F_i and power losses $N_{Ck\text{-}r}$. **Figures 4 and 5** show that, for different eccentricity deviations δ_e, the distribution of intertooth clearance Δ_i is different, regardless of the type of gearing.

For epicycloidal gearing, the following eccentricity deviations δ_e were considered:

- Positive deviation δ_e, i.e. $\delta_e > 0$, which means that the obtained value of eccentricity e is greater than its nominal value, the horizontal axis of the gear with the epicycloidal outline is shifted upwards in relation to the cooperating gear;
- Negative deviation δ_e, i.e. $\delta_e < 0$, which means that the obtained value of eccentricity e is smaller than its nominal value, the horizontal axis of the gear with the epicycloidal outline is shifted downwards in relation to the cooperating gear; and,
- eviation $\delta_e = 0$, which means that the obtained value of eccentricity e is equal to its nominal value, the position of the horizontal axes of the gears remains unchanged and are offset from each other with an eccentricity e.

Considering the epicycloidal gearing with a positive deviation δ_{ze} of its outline (**Fig. 4a**) and with its negative deviation δ_{ze} (**Fig. 4b**), it is noted that, for positive eccentricity deviation δ_e, intertooth clearance Δ_i increases from the minimum value for the first pair of teeth to the maximum value for the last pair. However, if the eccentricity deviation δ_e is negative, intertooth clearance Δ_i decreases from the maximum value for the first pair of teeth to the minimum value for the last pair of teeth. In turn, in the absence of eccentricity deviation, i.e. $\delta_e = 0$, the differences in the clearance distribution Δ_i for individual gearing can be seen. In the case of a positive gearing deviation δ_{ze} (**Fig. 4a**), clearance Δ_i for the first pair of teeth reaches the maximum value, then decreases, reaching the minimum value for one of the pairs, in order to grow for the next pairs, reaching again the maximum value for the last pair. In the case of a negative gearing deviation δ_{ze} (**Fig. 4b**), intertooth clearance Δ_i for the first pair of teeth reaches the minimum value, and then it grows reaching the maximum value for one of the pairs, and in turn for the next pairs decrease, reaching again the minimum value for the last pair.

In turn, for the hypocycloidal gearing, the following eccentricity deviations were considered δ_e:

- Positive deviation δ_e, i.e. $\delta_e > 0$, which means that the obtained value of eccentricity e is greater than its nominal value, the horizontal axis of the gear with the rollers is shifted downwards in relation to the cooperating gear;
- Negative deviation δ_e, i.e. $\delta_e < 0$, which means that the obtained value of eccentricity e is smaller than its nominal value, the horizontal axis of the gear with the rollers is shifted upwards in relation to the cooperating gear; and,
- Deviation $\delta_e = 0$, which means that the obtained value of eccentricity e is equal to its nominal value, the position of the horizontal axes of the gears remains unchanged and are offset from each other with an eccentricity e.

In the case of hypocycloidal gearin*g (**Fig. 5**), similarities in the change in clearance Δ_i to its changes for epicycloidal gearing can be seen with the difference that they occur for opposite deviations of the outline.

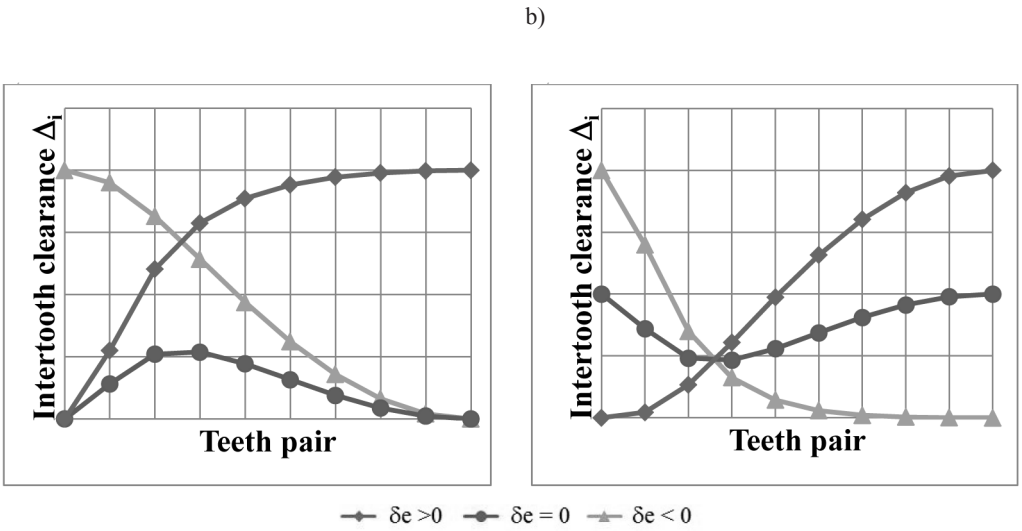

Fig. 5. The distribution of intertooth clearances Δ_i for hipocycloidal gearing with: a) a positive deviation δ_{zh}, b) a negative deviation δ_{zh}

Rys. 5. Rozkład luzów międzyzębnych Δ_i dla hipocykloidalnego zazębienia z: a) dodatnią jego odchyłką δ_{zh}, b) ujemną jego odchyłką δ_{zh}

Therefore, for a hypocycloidal outline with a positive deviation δ_{zh} (**Fig. 5a**), changes in this clearance are similar to changes in the epicycloidal outline with a negative deviation δ_{ze} (**Fig. 4a**). Moreover, changes in clearance Δ_i for a hypocycloidal outline with a negative deviation δ_{zh} (**Fig. 5b**) are similar to changes in the epicycloidal outline with a positive deviation δ_{ze} (**Fig. 4b**). In both cases, in relation to the outline deviations, the influence of the positive eccentricity deviation δ_e of the hypocycloidal outline on the clearance distribution Δ_i is identical to the positive deviation for the epicycloidal outline. A similar effect on clearance Δ_i has a negative eccentricity deviation δ_e for the hypocycloid outline and a negative deviation for the epicycloidal outline.

The distribution of intertooth clearance Δ_i, and thus manufacturing deviations, has a significant impact on the change in the number of teeth pairs cooperating with each other and the value of intertooth forces F_i. **Fig. 6 and Fig. 8** show the influence of the considered eccentricity deviation δ_e and the outlines deviations δ_{ze}, and δ_{zh} on distribution of intertooth forces F_i in cycloidal gearing. Additionally, the distribution of intertooth forces F_i was placed on them for transmission in which all the elements making the gearing do not have deviations (without clearance). **Fig. 6** shows the distribution of forces F_i for epicycloidal gearing.

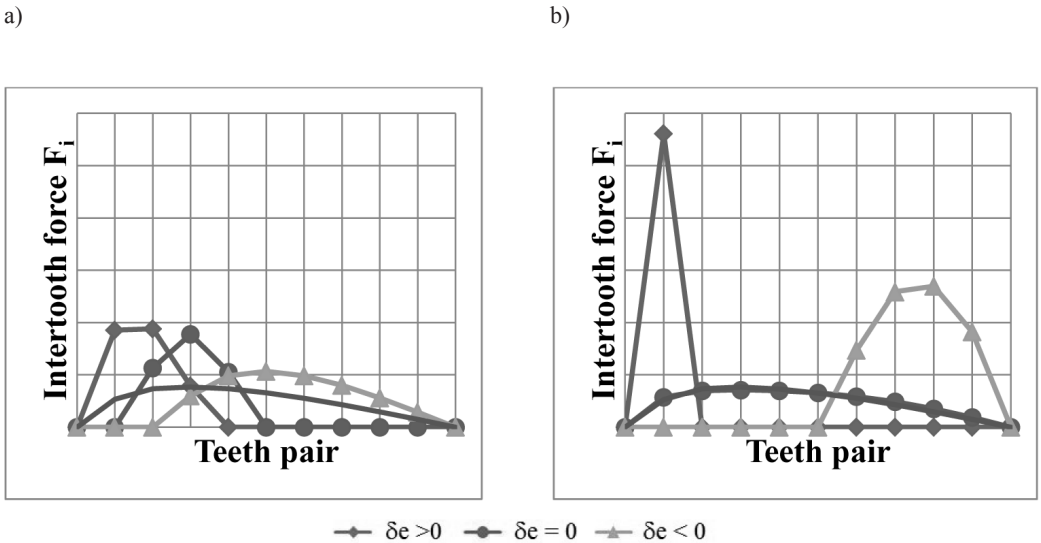

Fig. 6. Distribution of F_i forces in epicycloidal gearing: a) positive gearing deviation δ_{ze}, b) negative gearing deviation δ_{ze}

Rys. 6. Rozkład sił F_i w zazębieniu epicykloidalnym: a) dodatnia odchyłka uzębienia δ_{ze}, b) ujemna odchyłka uzębienia δ_{ze}

It can see that, regardless of whether the outline is with a positive deviation δ_{ze} (**Fig. 6a**), or with a negative one δ_{ze} (**Fig. 6b**), there is a clear impact of positive and negative eccentricity deviation δ_e causing a reduction in the number of teeth pairs cooperating with each other. If the eccentricity deviation δ_e is positive, then the initial teeth pairs work together, and when it is negative, the cooperation takes place for the final teeth pair. The reduction in the number of teeth pairs in gearing causes that the force values F_i in these pairs are definitely higher than in the teeth pairs for clearance-free transmission. This is particularly visible in the transmission in which the epicycloidal outline was made with a negative deviation δ_{ze}, i.e. $\delta_{ze} < 0$ (**Fig. 6b**).

Results obtained analytically (**Fig. 6**) were verified by the elastooptic method by studying the state of stress in a set of gears subjected to a given load [**L. 20**]. The aim of the research was to determine the teeth pairs that are in cooperation with each other. These tests involve the determination of isochromes in places where stress occurs, i.e. in the places where the outline of the gear is in contact with the rollers. For this purpose, the test gears were cast from an epoxy resin. **Fig. 7** shows the isochrome view for epicycloidal gearing with negative gearing deviation δ_{ze}, that is, the outline of the gear is smaller than the outline of the nominal gear and arose as a result of the shrinkage of the cast gear. The cooperating gear was created by casting the roller with the ring as one element. In this case, there was also a shrinkage causing the rollers to have a smaller diameter value. During the tests, a positive (**Fig. 7a**) and negative (**Fig.7b**) deviation δ_e was taken into consideration. The change in the axis distance of both cooperating gears (eccentricity *e*) was obtained by moving the gear with the rollers in the vertical plane. Moving the gear down, an eccentricity *e* was obtained with a positive deviation δ_e ($\delta_e > 0$). By doing the opposite, the eccentricity *e* was obtained with its negative deviation δ_e ($\delta_e < 0$). In the case of **Fig. 7a**, in which gears with positive eccentricity deviation δ_e ($\delta_e > 0$) were tested, it can be seen that the initial teeth pairs touch each other, which corresponds to the distribution of clearances Δ_i from **Fig. 4b** and forces F_i from **Fig. 6b**, for $\delta_{ze} < 0$ and $\delta_e > 0$. While, in the case of **Fig. 7b**, in which the gears with the negative eccentricity deviation δ_e ($\delta_e < 0$) were tested, it can be noticed that the middle and final pairs of teeth work together, which corresponds to the distribution of clearances Δ_i from **Fig. 4b** and forces F_i from **Fig. 6b**, for $\delta_{ze} < 0$ and $\delta_e < 0$. Therefore, it can be stated that the results from the tests coincide with the results obtained through the analytical method.

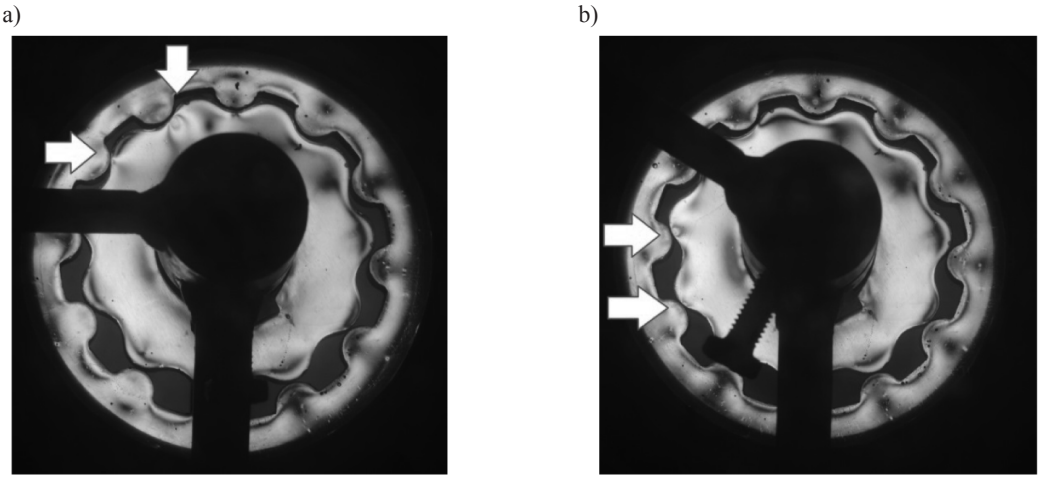

Fig. 7. Isochrome view of a set of gears with an epicycloidal gearing for: a) positive deviation of the eccentric ($\delta_e > 0$), b) negative deviation of the eccentric ($\delta_e < 0$)

Rys. 7. Widok izochrom w zespole kół z zazębieniem epicykloidalnym dla: a) dodatniej odchyłki mimośrodu ($\delta_e > 0$), b) ujemnej odchyłki mimośrodu ($\delta_e < 0$)

Figure 8 shows the distribution of forces F_i for hypocycloidal gearing, where **Fig. 8a** concerns the gearing with its positive deviation δ_{zh}, and **Fig. 8b** refers to the gearing with its negative deviation δ_{zh}. Similarly to the epicycloidal gearing, the effect of eccentricity deviation δ_e on the number of teeth pairs working together is clear. If the eccentricity deviation δ_e is positive ($\delta_e > 0$), then the initial pairs of teeth work with each other, and when it is negative ($\delta_e < 0$), then cooperation occurs for the final pair of teeth. The reduction in the number of teeth pairs in gearing causes that the forces values F_i in these pairs are definitely higher than in the teeth pairs for clearance-free transmission. This is particularly visible in the transmission in which the hypocycloidal outline was made with a positive deviation δ_{zh}, i.e. $\delta_{zh} > 0$ (**Fig. 8a**).

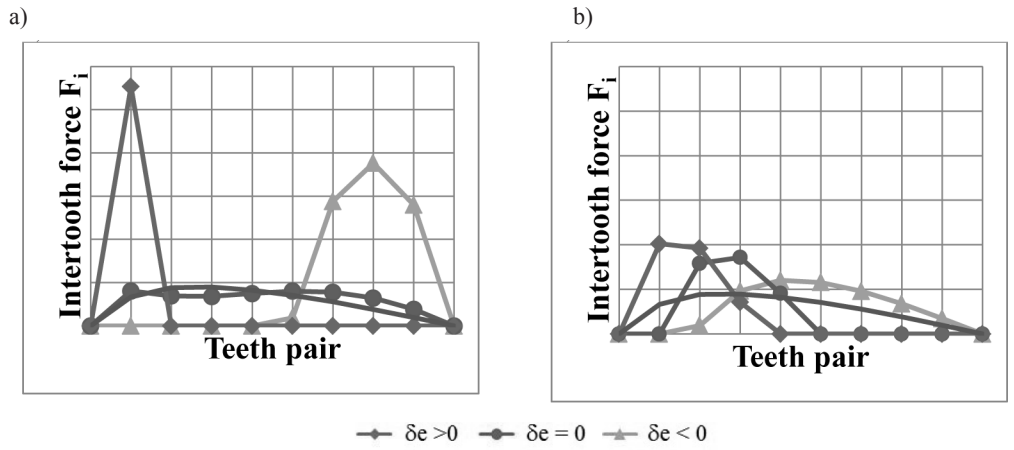

Fig. 8. Distribution of F_i forces in hypocycloidal gearing a) positive gearing deviation δ_{zh}, b) negative gearing deviation δ_{zh}
Rys. 8. Rozkład sił F_i w zazębieniu hipocykloidalnym a) dodatnia odchyłka uzębienia δ_{zh}, b) ujemna odchyłka uzębienia δ_{zh}

Figure 9 shows the isochrome view of the gear set with hypocycloidal gearing in which the hypocycloidal outline had a positive manufacturing deviation δ_{zh}. The casting shrinkage also occurred in both gears. In the case of positive eccentricity deviation δ_e ($\delta_e > 0$), the initial teeth pairs cooperate with each other (**Fig. 9a**). Moving a gear with a hypocycloidal profile downward, an eccentricity e was obtained with a positive deviation δ_e ($\delta_e > 0$). For the negative eccentricity deviation δ_e ($\delta_e < 0$), it can be seen that the contact between the outline and the rollers occurs for the final teeth pairs (**Fig. 9b**). In this case, the gear with the hypocycloidal outline was moved upward to obtain the eccentricity e with its negative deviation δ_e ($\delta_e < 0$). The results of the tests coincide with the results obtained through the analytical method (**Fig. 8a**).

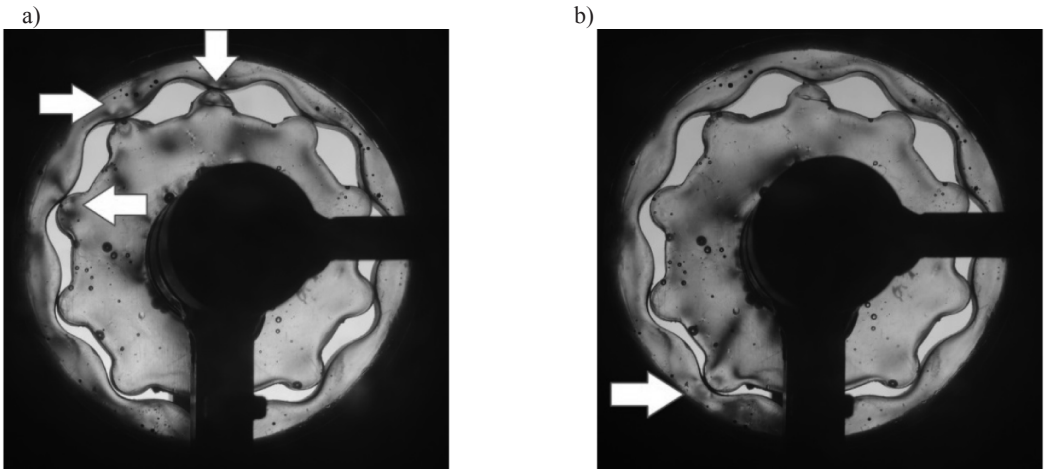

Fig. 9. Isochrome view of a set of gears with a hypocycloidal gearing for: a) positive deviation of the eccentric ($\delta_e > 0$), b) negative deviation of the eccentric ($\delta_e < 0$)
Rys. 9. Widok izochrom w zespole kół z zazębieniem hipocykloidalnym dla: a) dodatniej odchyłki mimośrodu ($\delta_e > 0$), b) ujemnej odchyłki mimośrodu ($\delta_e < 0$)

Figure 10 shows the influence of eccentricity deviation δ_e on the distribution of power losses $N_{Ck\text{-}r}$ in teeth pairs for epicycloidal gearing, and for hypocycloidal gearing in **Fig. 11**. In addition, a distribution of power losses for the transmissions with clearance-free gearing was placed on them.

Analysing these graphs, it can be clearly seen that the power losses $N_{Ck\text{-}r}$ in the gearing are dependent on the distribution of intertooth forces F_i, which is shown respectively for the epicycloidal gearing in **Fig. 6** and for the hypocycloidal gearing in **Fig. 8**. Power losses $N_{Ck\text{-}r}$ occur in places where intertooth forces F_i occur, since, at these points, the outline comes into contact with the rollers. In the case of positive eccentricity deviation δ_e ($\delta_e > 0$), these will be the initial teeth pairs for both epicycloidal and hypocycloidal gearing. Considering the negative eccentricity deviation δ_e ($\delta_e < 0$), it is concluded that power losses $N_{Ck\text{-}r}$ occurs in final pairs for both types

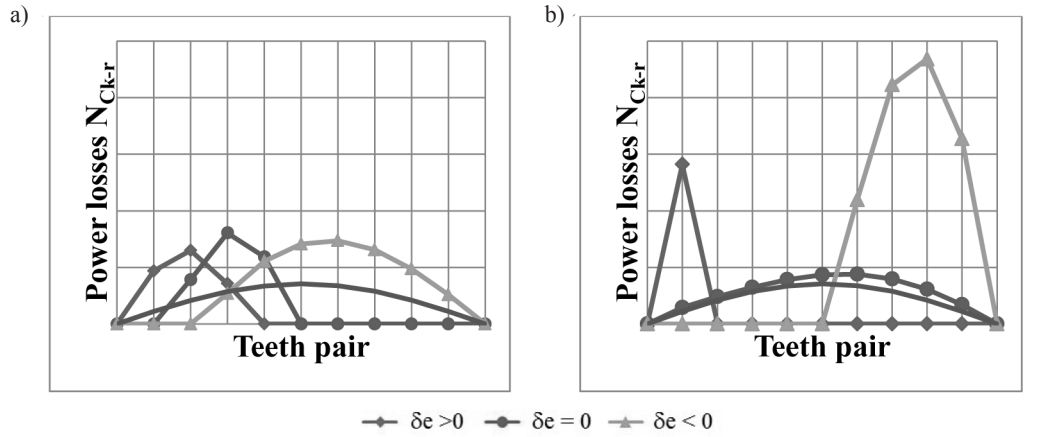

Fig. 10. Distribution of power losses N_{Ck-r} for epicycloidal gearing with: a) a positive deviation δ_{ze}, b) a negative deviation δ_{ze}
Rys. 10. Rozkład strat mocy N_{Ck-r} dla epicykloidalnego zazębienia z: a) dodatnią jego odchyłką δ_{ze}, b) ujemną jego odchyłką δ_{ze}

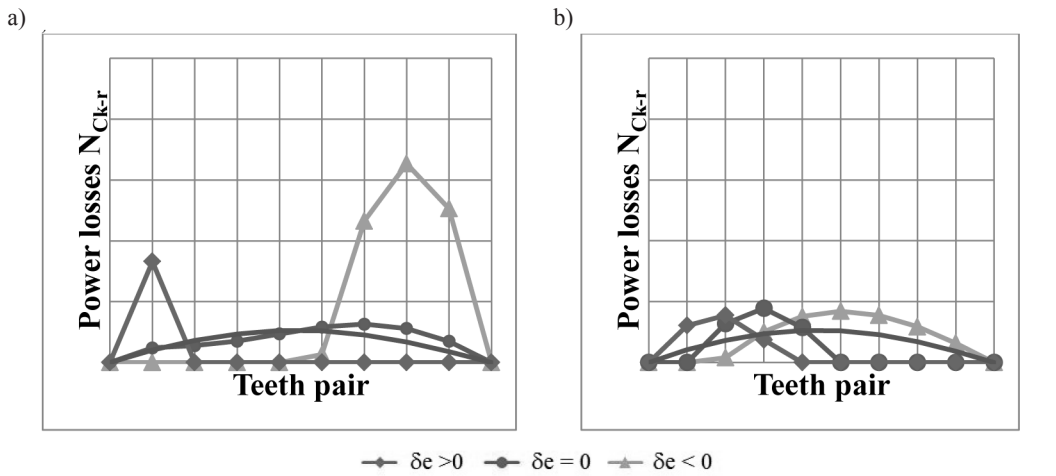

Fig. 11. Distribution of power losses N_{Ck-r} for hypocycloidal gearing with: a) a positive deviation δ_{zh}, b) a negative deviation δ_{zh}
Rys. 11. Rozkład strat mocy N_{Ck-r} dla hipocykloidalnego zazębienia z: a) dodatnią jego odchyłką δ_{zh}, b) ujemną jego odchyłką δ_{zh}

of gearing. In turn, for eccentricity e with nominal value ($\delta_e = 0$), power losses N_{Ck-r} will usually appear in the middle teeth pairs.

In most of the considered cases, the sum of losses N_{Ck-r} in cycloidal gearing is often greater than the sum of losses N_{Ck-r} for clearance-free transmissions. This sum may be smaller, usually when a small number of initial teeth pairs transfer the load.

SUMMARY

The article presents the influence of the eccentricity manufacturing deviation δ_e on the distribution of clearances Δ_i, intertooth forces F_i and power losses N_{Ck-r} in cycloidal gearing. This effect was considered for cases in which the cycloidal gear outline (epi- and hypo-) is made with a positive and negative manufacturing deviation δ_{ze}, and δ_{zh}. The distribution of intertooth clearance Δ_i is not the same and does not take constant values in individual teeth pairs. The analysis made it possible to determine the number of teeth pairs subjected to simultaneous loading or to indicate teeth pairs that do not engage in gearing at all, as shown by the distribution of intertooth forces F_i. The results of the calculations indicate that the impact of the eccentricity manufacturing deviation δ_e on the distribution of intertooth forces F_i is significant. The results obtained by an analytical method were verified by the elasto-optical method by studying the state of stress in gears set subjected to a given load. They are similar to each other. The distribution of power losses N_{Ck-r} in gearing is closely related to the distribution of intertooth forces F_i depending on the eccentricity deviation δ_e and has a very similar character. In most of the considered cases, the sum of losses N_{Ck-r} in cycloidal gearing is often greater than the sum of losses N_{Ck-r} for clearance-free transmissions. This sum may be smaller, usually when a small number of initial teeth pairs transfer the load.

REFERENCES

1. Hwang Y.W., Hsieh C.F.: Geometry Design and Analysis for Trochoidal·Type Speed Reducers: with Conjugate Envelopes. Transactions of the Canadian Society for Mechanical Engineering, vol. 30, No. 2, 2006, pp. 261÷278.
2. Warda B., Duda H.: A Method for Determining the Distribution of Loads in Rolling Pairs in Cycloidal Planetary Gear, Tribologia 1/2017, pp. 105–111.
3. Chmurawa M., John A.: Numerical analysis of forces, stress and strain in planetary wheel of cycloidal gear using FEM, Numer. Methods Contin. Mech. Liptovsky Jan. Slovak Repub., 2000.
4. Biernacki K., Stryczek J.: Analysis of stress and deformation in plastic gears used in gerotor pump, The journals of Strain Analysis for Engineering Design, vol. 45, issue 7, 2010, pp. 465–479.
5. Blanche J.G., Yang D.C.H.: Cycloid Drives with Machining Tolerances. ASME Journal of Mechanisms, Transmissions, and Automation in Design, vol. 111, No. 3, 1989, pp. 337–344.
6. Yang D.C.H., Blanche J.G.*:* Design and Application Guidelines for Cycloid Drives with Machining Tolerances. Mechanism and Machine Theory, vol. 25, No. 5, 1990, pp. 487–501.
7. Ivanovic L., Devedzic G., Cukovic S., Miric N.: Modeling of the Meshing of Trochoidal Profiles with Clearances. Journal of Mechanical Design, vol. 134, 2012, pp. 041003-1–041003-9.
8. Dudek A., Sendyka B.: Siły międzyzębne w przekładni obiegowej z zazębieniem cykloidalnym. Przegląd Mechaniczny, 1986, Nr 14, s. 3–6.
9. Xu L.X., Chen B.K., Li Ch..: Dynamic modelling and contact analysis of bearing-cycloid-pinwheel transmission mechanisms used in joint rotate vector reducers. Tolerances. Mechanism and Machine Theory, vol. 137, 2019, pp. 432–458.
10. Gorla C., Davoli P., Rosa F., Longoni C., Chiozzi F., Samarini A.: Theoretical and experimental analysis of a cycloidal speed reducer. ASME Journal of Mechanical Design, 2008, 130.
11. Mackic T., Blagojevic M., Babic Z., Kostic N.: Influence of design parameters on cyclo drive efficiency, Journal of the Balkan Tribological Association, vol. 19, No. 4, 2013, pp. 497–507.
12. Sensinger J.: Unified Approach to Cycloid Drive Profile, Stress, and Efficiency Optimization. ASME Journal of Mechanical Design, vol. 132, 2010, pp. 024503-01–024503-05.
13. Cichocki W.: Tarcie i opory ruchu w wybranych parach kinematycznych przekładni typu CYCLO. Prace Komisji Mechaniki Stosowanej, Mechanika, Nr 14/1990. Wyd. PAN – Oddział w Krakowie, Kraków 1990, s. 7–23.
14. Stryczek J.: Projektieren der Zykloidenverzahnungen hydraulischer Verdrangermaschinen, Mechanism and Machine Theory, vol. 25, No. 6, 1990, pp. 597–610.
15. Blagojevic M.: Analysis of Clearances and deformations at Cycloid Disc. Machine Design, vol.6, No.3, 2014, pp. 79–84.
16. Sun Y., Guan T.: The Modeling and Simulation Method to Calculate Force in the Equivalent Substitution Flank Profile Two Tooth Difference Cycloid Pin Gear Reducer Cycloid Gear, International Conference on Digital Manufacturing & Automation, 2010, Changcha, Hunan China, pp. 729–733.
17. Guangwu Z., at al.: Mixed lubrication analysis of modified cycloidal gear used in the RV reducer, Journal of Engineering Tribology, vol. 230, No. 2, 2016, pp. 121–134.
18. Bednarczyk S.: Designing the Hypocycloidal Gearing in the Planetary Transmission. Machine Dynamics Research, Vol. 39, No. 3, 2015, pp. 5–23.
19. Bednarczyk S.: Analysis of the Possibility of Applying Epi- and Hypocycloid in Planetary Transmissions. Machine Dynamics Research, Vol. 41, No. 1, 2017, pp. 113–128.
20. Orłoś Z.: Doświadczalna analiza odkształceń i naprężeń, PWN, Warszawa, 1977.